Sensors & Actuators: B. Chemical 272 (2018) 236–242

Contents lists available at ScienceDirect

Sensors and Actuators B: Chemical

journal homepage: www.elsevier.com/locate/snb

Sezawa wave acoustic humidity sensor based on graphene oxide sensitive film with enhanced sensitivity

I.E. Kuznetsova[a,*], V.I. Anisimkin[a], V.V. Kolesov[a], V.V. Kashin[a], V.A. Osipenko[b], S.P. Gubin[c], S.V. Tkachev[c], E. Verona[a,d], S. Sun[e], A.S. Kuznetsova[a]

[a] Kotelnikov Institute of Radio Engineering and Electronics of RAS, Moscow, 125009, Russia
[b] OAO "NII Elpa", Zelenograd, Moscow, 124460, Russia
[c] Kurnakov Institute of General and Inorganic Chemistry of RAS, Moscow, 119991, Russia
[d] Institute for Photonics and Nanotechnologies, IFN-CNR, Via Cineto Romano 42, 00156 Rome, Italy
[e] Management School, University of Shanghai for Science and Technology, 516 Jungong Road, Shanghai 200093, PR China

ARTICLE INFO

Keywords:
Humidity sensor
Sezawa wave
Piezoelectric structures
Multilayered waveguide
ZnO film
Graphene oxide film

ABSTRACT

The measurement of humidity is very important for air control in ambient, industry, cars, houses, closed apartments, museums, atomic power stations, etc. In the present work the theoretical analysis of the surface acoustic wave propagation in "graphen oxide (GO) film/ZnO film/Si substrate" layered structure has been performed. The change of GO film conductivity due to humidity has been taken into account during the calculations. Based on the obtained results an improved microwave acoustic humidity sensor has been developed. The sensor has enhanced sensitivity of about 91 kHz/% and linear response vs relative humidity in the range 20–98%RH. It is based on the mode belonging to Sezawa wave family that is shown to be more sensitive towards electric conductivity variations in GO film produced by adsorbed water molecules than the Rayleigh counterpart.

1. Introduction

In recent years the microwave acoustic humidity sensors have been developed very extensively [1–26]. These sensors are successfully used for air control in ambient, industry, cars, houses, closed apartments, museums, atomic power stations, etc. [27,28]. For development of the humidity sensors various types of acoustic waves (surface (SAW) [1–11], Love [12–17], bulk [18–24], and Lamb [25,26]) have been used. These waves propagated either in homogeneous crystal substrates or in multi-layered structures containing different sorbent films sensitive towards water vapor adsorption. Usually, the sensitive films are made of ceramic, semiconducting and polymer materials [28,29]. In recent years they are fabricated from graphen-based layers [5–7,17,20–23,25,26,30–32] or special materials doped by nano-particles, fullerens, and carbon nano-tubes [8–11,14,17,24]. For any sorbent material adsorption of water molecules produces, in general, the changes in film density, elasticity, electric conductivity, dielectric permittivity, and temperature, which are detected at the output of the sensor as the changes in acoustic wave velocity, frequency, phase and/or amplitude. However, usually, designers use the film with one dominant sensing mechanism. For example, the GO layer with dominant electric conductivity variations, allowed to develop recently the super-high-sensitive humidity sensor based on high-order (symmetric) Lamb mode in 128Y,X + 90^0 − $LiNbO_3$ plate [26].

In spite of large amount of paper devoted to humidity sensors, further improvements in the sensors performance are still strongly required making new researches and developments in the field actual.

The goal of the present paper is to develop improved humidity sensor basing on theoretical analysis and experimental verification of the acoustic waves propagation in "GO film − ZnO film − Si substrate" layered structure.

2. Theoretical analysis

Propagation of the acoustic waves is studied in two dimensional structures with x_1- axis parallel to the propagation direction and x_3- axis perpendicular to the structure surface (Fig. 1). On Fig. 1,a the regions $x_3 < -h_1$, $-h_1 < x_3 < 0$ and $x_3 > 0$ are occupied, respectively, by air, ZnO film and Si half-space. On Fig. 1,b air is for $x_3 < -h_2$, while $-h_2 < x_3 < -h_1$ is for the GO film. Mechanical and electrical variables are assumed to be constant in the x_2-axis direction.

To solve the problem we write motion Eq. (1), Laplace (2) or Puasson (3) equations, continuity equation for electric charge (4), and material Eqs. (5)–(8) for GO, ZnO and Si medium using the quasi-

* Corresponding author at. Contact Iren E. Kuznetsova, Mokhovaya 11, bld.7, Kotelnikov Institute of Radio Engineering and Electronics of RAS, Moscow, 125009, Russia.
E-mail address: kuziren@yandex.ru (I.E. Kuznetsova).

https://doi.org/10.1016/j.snb.2018.05.158
Received 19 February 2018; Received in revised form 14 May 2018; Accepted 26 May 2018
Available online 28 May 2018
0925-4005/

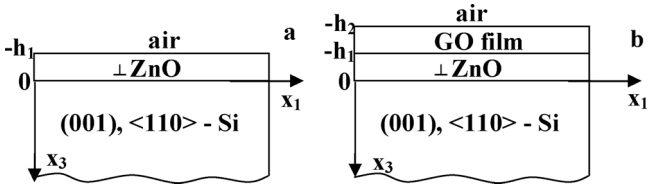

Fig. 1. Geometry of the problems. (a) ZnO/Si structure, (b) GO/ZnO/Si structure.

electrostatic approximation $E_i = \partial\Phi/\partial x_i$ [33]:

$$\rho^{Si,GO,ZnO}\partial^2 U_i/\partial t^2 = \partial T_{ij}/\partial x_j, \tag{1}$$

$$\partial D_j^{Si,ZnO}/\partial x_j = 0, \tag{2}$$

$$\partial D_j^{GO}/\partial x_j = -\delta_v^{GO}, \tag{3}$$

$$\partial J_i^{GO}/\partial x_i + \partial\delta_v^{GO}/\partial t = 0, \tag{4}$$

$$T_{ij}^{Si,GO} = C_{ijkl}^{Si,GO}\partial U_l/\partial x_k, \quad D_j^{Si,GO} = -\varepsilon_{jk}^{Si,GO}\partial\Phi/\partial x_k, \tag{5}$$

$$J_i^{GO} = -\sigma_v^{GO}\partial\Phi/\partial x_i + d^{GO}\partial\sigma_v^{GO}/\partial x_i, \tag{6}$$

$$T_{ij}^{ZnO} = C_{ijkl}^{ZnO}\partial U_l/\partial x_k + e_{kij}^{ZnO}\partial\Phi/\partial x_k, \tag{7}$$

$$D_j^{ZnO} = -\varepsilon_{jk}^{ZnO}\partial\Phi/\partial x_k + e_{jlk}^{ZnO}\partial U_l/\partial x_k \tag{8}$$

Here, E_i, U_i, J_i, t, T_{ij}, x_j, D_j, Φ, ρ, C_{ijkl}, e_{ikl}, ε_{jk}, δ_V, σ_V and d are the components of the electric field, mechanical particle displacement, electrical current, time, the components of mechanical stress tensor, coordinates, the components of electric displacements, electrical potential, and density, as well elastic, piezoelectric and dielectric constants, bulk charge, bulk conductivity, and diffusion coefficient of a materal, respectively. Indexes ZnO, Si, and GO are attributed to different materials.

Outside the plate ($x_3 < -h_1$, Fig. 1,a; $x_3 < -h_2$, Fig. 1,b) electric displacement of the waves satisfies the Laplace equation:

$$\partial D_j^{ar}/\partial x_j = 0, \tag{9}$$

where $D_j^{ar} = -\varepsilon^{ar}\partial\Phi^{ar}/\partial x_j$, index *ar* denotes air, ε^{ar} is the air dielectric constant.

Additionally, the waves satisfy mechanical and electrical boundary conditions:

– for structure on Fig. 1a they are

$$x_3 = 0: \ T_{3j}^{Si} = T_{3j}^{ZnO}, \ \Phi^{Si} = \Phi^{ZnO}; \ D_3^{Si} = D_3^{ZnO}. \tag{10}$$

$$x_3 = -h_1: \ T_{3j}^{ZnO} = 0, \ \Phi^{ZnO} = \Phi^{ar}; \ D_3^{ZnO} = D_3^{ar}. \tag{11}$$

– for structure on Fig. 1b they are

$$x_3 = -h_1: \ T_{3j}^{ZnO} = T_{3j}^{GO}, \ \Phi^{ZnO} = \Phi^{GO}, \ D_3^{ZnO} = D_3^{GO}, \ J_3^{GO} = 0 \tag{12}$$

$$x_3 = -h_2: \ T_{3j}^{GO} = 0, \ \Phi^{GO} = \Phi^{ar}, \ D_3^{GO} = D_3^{ar}, \ J_3^{GO} = 0. \tag{13}$$

Using relevant equations and boundary conditions, the problem of acoustic wave propagation is solved as follows. The solution is presented in the form of a set of plane inhomogeneous waves [34,35]:

$$Y_i(x_1, x_3, t) = Y_i(x_3)\exp[j\omega(t - x_1/V_{ph})], \tag{14}$$

where i = 1–8 for the ZnO, i = 1–6 for the mechanical part of task for Si and GO, and i = 1, 2 for air and electrical part of task for Si and GO, V_{ph} is phase velocity, and ω – is the angular frequency of an acoustic wave.

Then, the normalization is introduced as follows:

$$Y_i = \omega C_{11}^* U_i/V_{ph}, \ Y_4 = T_{13}, \ Y_5 = T_{23}, \ Y_6 = T_{33}, \ Y_7 = \omega e^*\Phi/V_{ph}, \ Y_8 = e^* D_3/\varepsilon_{11}^*, \tag{15}$$

where i = 1,2,3, C_{11}^*, ε_{11}^* are the normalized material constants of ZnO, Si and GO in crystallographic coordinate system; e^* = 1 and it has the dimensional representation of piezoelectric constant.

Substituting (14) in (1)–(8) yields a system of 8, 6, 6, 4 and 2 conventional differential linear equations for ZnO, Si (mechanical part), GO (mechanical part), Si (electrical part), GO (electrical part) and air, respectively, where each system can be written in the matrix form:

$$[A][dY/dx_3] = [B][Y]. \tag{16}$$

Here $[dY/dx_3]$ and $[Y]$ are 8, 6, 6, 4 and 2 dimensional vectors for ZnO, Si (mechanical part), GO (mechanical part), Si (electrical part), GO (electrical part) and air, respectively, whose components are defined according the formulae (15). Matrixes $[A]$ and $[B]$ appeared to be squared and have dimensions of 8 x 8 for ZnO, 6 × 6 for Si and GO (mechanical part), 4 × 4 GO (electrical part), and 2 × 2 for Si and air.

Since matrix $[A]$ is not particular ($det[A] \neq 0$) we can write the following equations for every contacting medium:

$$[dY/dx_3] = [A-1][B][Y] = [C][Y] \tag{17}$$

After that, to solve the system of Eq. (17) we need to find the eigenvalues $\beta^{(i)}$ of matrices $[C]$ and corresponding eigenvectors $[Y^{(i)}]$, responsible for the parameters of partial waves, for each of contacting media. General solution would be a linear combination of all partial waves for each medium:

$$Y_k = \sum_{i=1}^{N} A_i Y_k^{(i)}\exp(\beta^{(i)}x_3)\exp(j\omega[t - x_1/V_{ph}]), \tag{18}$$

where the number of eigenvalues N is 8 for ZnO, N = 6 for Si and GO (mechanical part), N = 4 for GO (electrical part), N = 2 for Si and air. Unknowns A_i and phase velocity V_{ph} can be found using mechanical and electrical boundary conditions (10)–(13) that have also been written in the normalized form (15).

Moreover, as all variables should decay into Si substrate the eigenvalues with positive real parts are eliminated from consideration for nonpiezoelectric half-space. Furthermore, only four eigenvalues with negative real parts are taken into account for the nonpiezoelectric medium, as well as all eigenvalues of corresponding matrix [C] for ZnO film ($0 > x_3 > -h_1$, Fig. 1a,b) and GO film ($-h_1 > x_3 > -h_2$, Fig. 1b).

Finally, since all variables must have decaying amplitudes in air we exclude the eigenvalues with the negative real parts for air ($x_3 < -h_1$, Fig. 1,a; $x_3 < -h_2$, Fig. 1,b). As a result, the described procedure allowed us to calculate the wave phase velocity in structures under the study.

The calculation of the electromechanical coupling coefficient is accomplished using well known formulae [33]:

$$k^2 = 2\frac{V_{ph} - V_{ph_m}}{V_{ph}} \times 100\%, \tag{19}$$

where $V_{ph_m}$is phase velocity of acoustic waves when the plane $x_3 = -h_1$ is electrically shorted.

3. Experimental

Silicon is well-known as one of the most popular and cheap material in modern electronics. Therefore, design of any, in particular, humidity sensors based on this material is very attractive. On the other hand, Si is not piezoelectric, while acoustic waves are usually generated by exploiting the piezoelectric effect. That is why the silicon substrate should be covered with a piezoelectric layer, say, ZnO film. However, this film itself is not very sensitive towards humidity [14,16]. Therefore, in designing acoustic wave humidity sensor, the other sorbent film above ZnO layer (e.g. GO film) should be additionally applied.

3.1. Preparation of graphene oxide suspension

As in our previous papers [26,36] the graphene oxide (GO) film was fabricated starting from China natural graphite (99.9% C). The material was grinded in a ball crusher 200–300 μm in diameter, oxidized [37], and dried for 6 h at 50–60 °C. After that 0.4–0.5 g of graphite oxide was placed in a cylinder chamber (250 ml) together with distilled water (150 ml) and sonicated (20.4 kHz, 0.1–1 W/sm^3) during 15 min. The as-obtained water dispersion with GO particles was centrifuged during 10 min at 8000 rev/min and dried at 70 °C for 6 h [38].

3.2. Design of the humidity sensor

Experimental sample represents common delay line implemented on (001),<110>-Si substrate (4.5 Ω/cm, 500 μm thick) and C_6-ZnO film (h_1 = 3 μm). Input and output interdigital transducers (IDT) (20 finger pairs) are made on the film by lift-off technique using V- Al film (0.03/0.3 μm, 1.15 Ω/cm). Period of the transducers is λ = 32.1 μm, the distance between them is L_{IDT} = 5 mm, aperture is equal 2 mm and the total phase acquiring an acoustic wave between input and output transducers is $\varphi_0 = 360^0(L_{IDT}/l) = 56\ 075^0$.

The fabrication of the c-oriented textured ZnO films with grains of about 0.3 μm is performed in triode sputtering system with dc current, ZnO target, 80% Ar + 20% O_2 gas mixture, and 0.07 Pa pressure. The substrate temperature is 250 °C. The rate of the sputtering is 1.2–3 μm per hour.

The GO-based dispersion was deposited onto ZnO film between IDTs by airgraph and dried at the room temperature for 24 h. The film was 2 × 2 mm^2 in square and 0.45 μm in thickness.

The scheme (a) and photo of the designed humidity sensor in a holder (b) are shown on Fig. 2.

The as-fabricated sample is tested by network analyser (Keysight E5061B). The type of the wave (Rayleigh/Sezawa) is identified from comparison of the calculated phase velocity V_{ph} with the experimental value determined as $V_{ph} = f \times \lambda$, where f is the wave central frequency and λ is the transducer period equal to the acoustic wavelength.

3.3. Measurement of humidity effect

The changes in characteristics of the Rayleigh and Sezawa waves produced by humidity are measured using experimental setup presented in Fig. 3 [26]. The delay line (DL) is fixed into the chamber (750 ml) and forced by laminar air flux (100 ml/min). Humidity in the flux is varied in the range RH = 3.6–98% by ratio between dry and humid air injected together. The value of the humidity is also controlled by commercial thermo-hygrometer IVTM-7 (threshold 0.1%) located near the tested sensor. The measurements are carried out at room temperature (22 °C).

The steps of the measurements are as follows. First, to avoid interaction of humid air with uncontrollable gaseous species preadsorbed on the surface and in the volume, the graphene oxide film was preliminary cleaned by dry nitrogen for about 5 min. Then, the nitrogen was switched off and dry air was introduced into the chamber as reference gas for about 2 min. Finally, the dry air was switched off, the humid air was switched on, and the acoustic response was measured towards dry air for as-cleaned film.

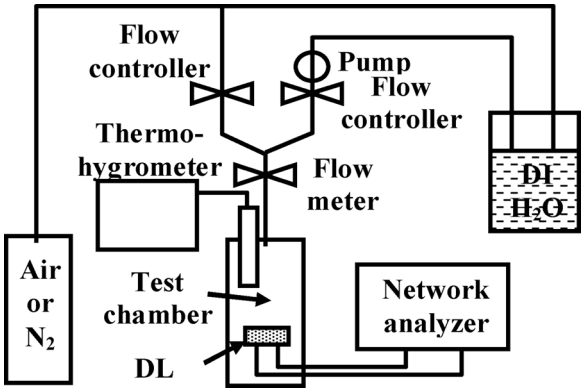

Fig. 3. Experimental setup for testing humidity sensor based on acoustic waves in GO/ZnO/Si structure.

The sensitivity of Rayleigh and Sezawa waves towards humidity is evaluated from the change in the phases Δφ measured at central frequency. In order to avoid dependence of the measurements on the length of the GO film (L_{GO}) the values of Δφ are normalized to the total phase $\varphi_0 = 360^0(L_{IDT}/l) = 56\ 075^0$ acquiring the wave between input and output transducers and multiplied to enhance factor (L_{IDT}/L_{GO}). As a result, the normalized responses $R = (\Delta\varphi/\varphi_0)(L_{IDT}/L_{GO})$ of the different waves could be compared with each other at identical experimental conditions.

3.4. Measurement of GO film conductivity

The measurement of the electric conductivity of the graphene oxide film was carried out using two-contact method and RF electric bridge (1 kHz) in hermetic box at room temperature and humidity ranged from 5 to 98%. The test sample (10 × 3 × 0.1 mm^3) was placed onto the glass substrate with its surface resistance $\Omega > > 10^{14}$ Ohm. At the ends of the sample two silver paste contacts ($\Omega < < 10^{-1}$Ohm) were fabricated. The results of the measurements were recalculated to specific resistance.

It was found that the conductivity of the GO film is increased from 10^{-4} S/m up to 5 S/m. Like in [39] this property may be attributed to the presence of hydroxyl and epoxy groups on the surface of graphene sheets and to absorption of the water molecules by carbonyl and carboxyl groups existing at the edges of sheets or defects.

4. Results and discussion

4.1. Theoretical results

At first step the SAW properties in ZnO/Si structure supporting

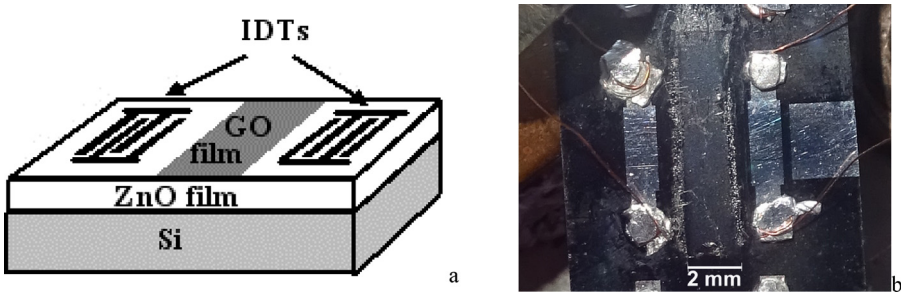

Fig. 2. (a) The scheme and (b) photo of the designed humidity sensor in a holder.

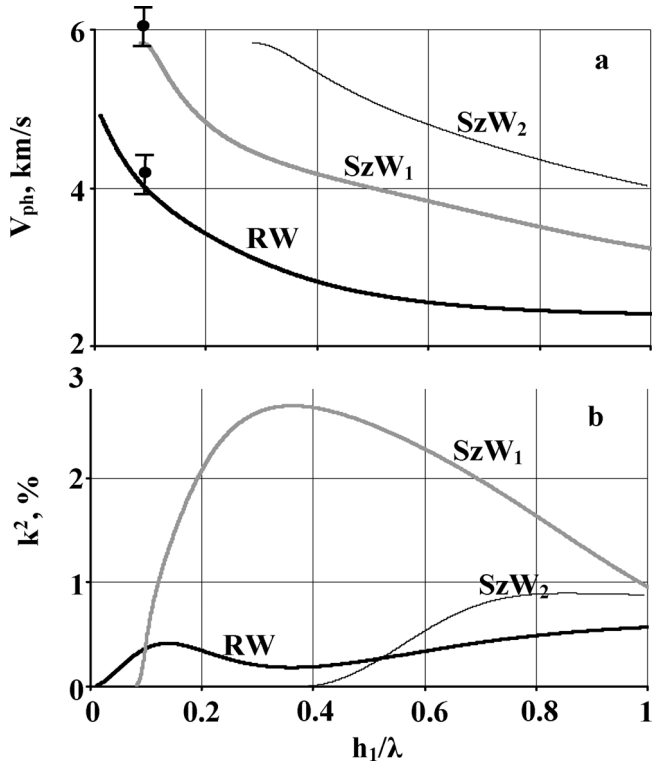

Fig. 4. (a) The phase velocity and (b) electromechanical coupling coefficient versus the thickness of ZnO film h_1/λ (λ is wavelength) in ZnO/Si structure. RW – Rayleigh wave; SzW_1, SzW_2–1st and 2nd Sezawa modes.

Rayleigh and Sezawa waves [40–42] are analyzed using material constants from [43] (Si) and [40,41] (ZnO) (Fig. 3). The crystal orientations are (001),<110> for Si (Eugler angles 0^0, 0^0, 45^0) and (001),<100> for ZnO (0^0, 0^0, 0^0).

Fig. 4 shows that for $h_1/\lambda > 0.1$ the k^2 of the 1st Sezawa mode is larger than that is for the Rayleigh wave. It is just this property that is exploited in present paper to improve sensitivity of the SAW humidity sensor based on GO sorbent film whose dominant sensing mechanism is related to the change in film conductivity as approved in [26] by 2 independent experiments. The first one showed that the response calculated from preliminary measured density, elastic modulii, and their changes is much lower than the value measured for the same GO film and substrate material – so that the contribution of the mechanical properties of the film is not the main. Second, the SAW humidity response was measured for one and the same GO film deposited on strong ($LiNbO_3$) and weak (quartz) piezoelectric substrates. It turned to be out that the former substrate ensured much higher response than the latter one – so that the dominant contribution is originated from electric properties of the film and electric fields of the SAW.

At second step the properties of the Rayleigh and Sezawa waves are examined for the same structure with additional GO film. The film is supposed to be isotropic. The material constants of the film at different relative humidities RH are taken from [26].

The calculations show that before humid air exposure ("clean" GO film) the velocities and $k^2$of the waves at $h_1(ZnO) = 3\,\mu m$, $h_2(GO) = 0.45\,\mu m$, and $h_2/h_1 = 0.15$ are $V_{ph}^{RW} = 3521.5$ m/s, $k^2 = 0.27\%$, and $V_{ph}^{SzW_1} = 5644.6$ m/s, $k^2 = 0.52\%$. After exposure (the film with water molecules), when the thickness of the GO film is doubled [26] ($h_2(GO) = 0.9\,\mu m$, $h_2/h_1 = 0.3$), the same velocities become larger: $V_{ph}^{RW} = 3546.4$ m/s and $V_{ph}^{SzW_1} = 5657.4$ m/s.

The increase of the velocities in this case is attributed to the large increase in the GO film thickness. On the other hand, for analyses accounting the increase in the GO film conductivity the effect of water vapor results to the decrease in the wave velocities: $V_{ph}^{RW} = 3511.4$ m/s and $V_{ph}^{SzW_1} = 5614.7$ m/s at $h_2/h_1 = 0.15$. Therefore, the responses of the waves towards humidity predicted by our calculations may be estimated as 0.3% and 0.53% at RH = 67%, respectively. The corresponding theoretical data are presented in Table 1.

Table 1
Results of the theoretical analysis.

h_2^{GO}, μm	h_2/h_1	RH,%	Taking into account only GO film thickness changes		Taking into account only GO conductivity changes (σ_V = 5 S/m)	
			V_{ph}^{RW}, m/s	V_{ph}^{SzW1}, m/s	V_{ph}^{RW}, m/s	V_{ph}^{SzW1}, m/s
0.45	0.15	0.47	3521.5	5644.6	3511.4	5614.7
0.6	0.2	26	3566.1	5651.5	3556.2	5629.2
0.84	0.28	56	3546.0	5650.1	3538.6	5628.1
0.9	0.3	67	3459.3	5641.5	3453.4	5611.5

The same calculation for the Lamb wave sensor and GO film/128Y-X + 90^0 structure [26] gives lower humidity response (0.05%) though the coupling coefficient k^2 of the wave is higher (10.3%). Such sort of contradiction may be explained by stronger energy concentration of the Rayleigh and Sezawa SAWs into GO film than that is for the Lamb wave distributed over the whole film/plate structure.

As a result, theoretical analysis accomplished in this chapter predicts that humidity sensor based on Sezawa wave and GO/ZnO/Si structure should provide better sensitivity than it was achieved before.

4.2. Experimental results

The measured transfer function $|S_{21}|$ of Rayleigh wave (1) and Sezawa family waves (2) in GO film/ZnO film/Si substrate layered structure is shown in Fig. 5. The central frequencies of the waves measured in experiment are, respectively, 134.75 MHz for Rayleigh wave and between 95 and 270 MHz for Sezawa waves. The measured velocities of the waves determined as described in Section 3.2 are 4300 ± 430 m/s (Rayleigh wave 1) and 6600 ± 660 m/s (Sezawa wave 2), where the experimental errors are estimated from precision of the frequency measurements suffered of $|S_{21}|$ ripples and of the averaged period of IDT perturbed by etching process. The family of Sezawa waves consists of a number of modes with various characteristics each.

As an example Fig. 6 demonstrates humidity responses of the Rayleigh (a, c) and Sezawa (b, d) waves measured in ZnO/Si (a,b) and GO/ZnO/Si (c,d) structures at RH ≈ 26%. Selected Sezawa wave has lowest insertion loss among other modes of the family. It is seen that i) responses of both waves much higher with GO film (c,d) than without it (a,b), ii) responses of Sezawa wave ($\Delta\varphi_{Sezawa} = -4.46^\circ, -161.42^\circ$) are larger than those are for Rayleigh wave ($\Delta\varphi_{Rayleigh} = -2.28^\circ, -16.48^\circ$)

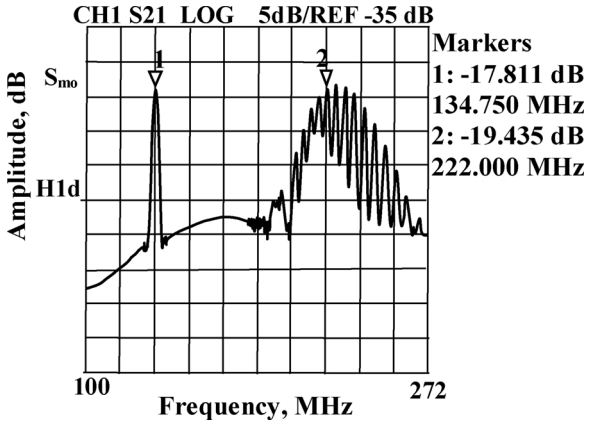

Fig. 5. Transfer function $|S_{21}|$ of Rayleigh wave (1) and one of Sezawa wave (2) in GO film/ZnO film/Si substrate layered structure.

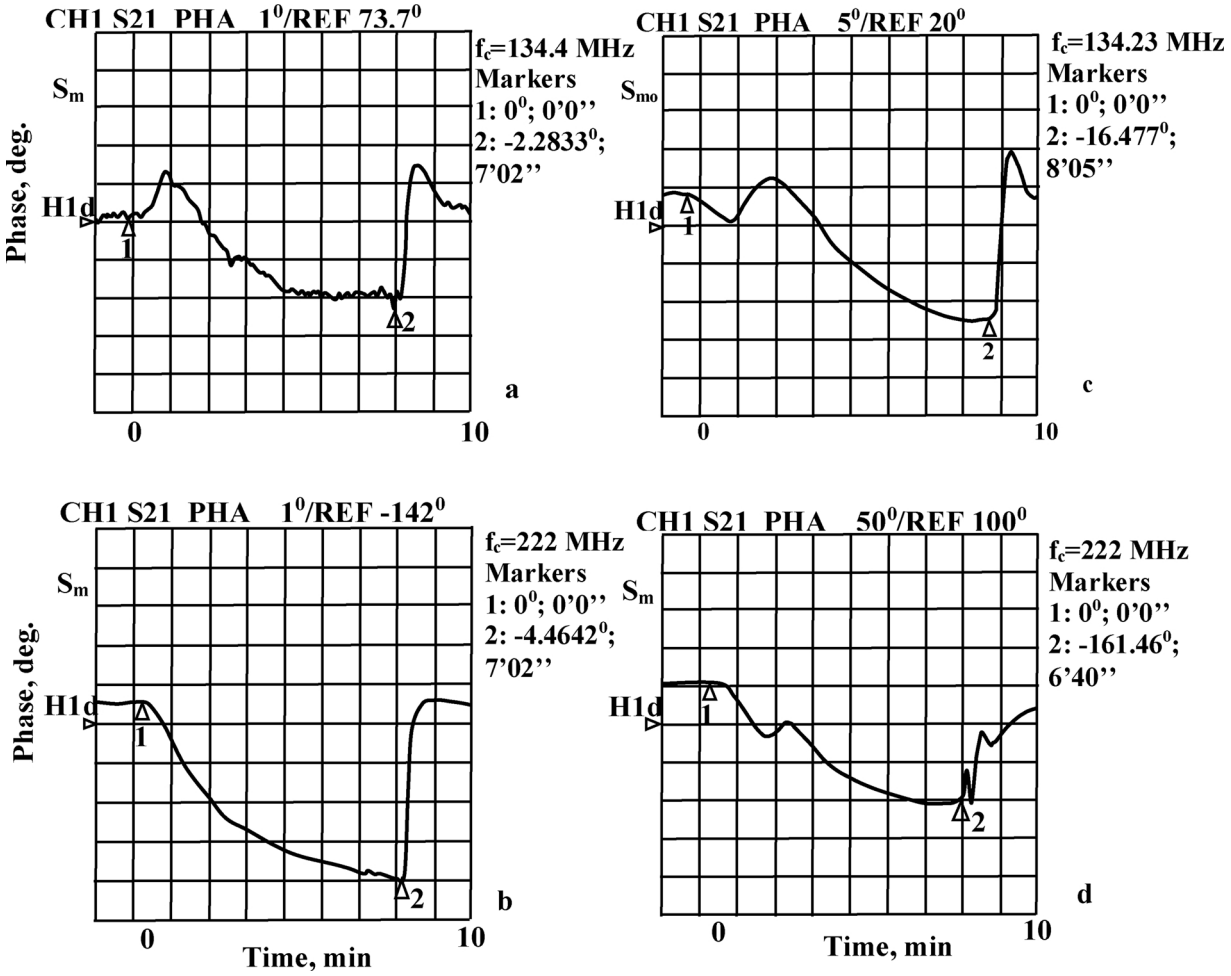

Fig. 6. Humidity responses vs time for (a, c) Rayleigh and (b, d) Sezawa waves measured in (a, b) ZnO/Si and (c, d) GO/ZnO/Si structures at RH ≈ 26%. f_c is the wave central frequency. 1 − dry air off, humid air on, 2–humid air off, dry air on.

for both test structures, iii) response times (≈ 600 s) are much longer than those are for recovery (≈ 6 s) for both structures and both waves. Analysis of the same values for the other humidity has shown that the values of the response/recovery times are increased from 500s/5 s at RH = 5% to 700s/18 s at RH = 98%. Like for hydrogen detection with polycrystalline Pd film [4] the large times may be attributed to the porous nature of the sensitive GO film making penetration of the adsorbed water species into the film volume quite difficult, iv) after switching humidity off the output signal restores completely, v) Rayleigh wave response is positive at the beginning and negative at its saturation indicating that the response of the wave is a combination of various sensing mechanisms.

Possible explanation for the initial increase in the Rayleigh wave velocity produced by water vapor adsorption (Fig. 6a,c) is the presence of two opposite sensing mechanisms [44]. On the one hand, the water molecules change mechanical properties of the GO film [26] and ZnO layer [44], i.e. the first mechanism is the elastic loading effect resulting to increase in the Rayleigh wave velocity. On the other hand, the water vapor adsorption increases the GO film conductivity and the mass loading [44] resulting to decrease in the wave velocity. As a result, at initial stage the first sensing mechanism is larger than the second one, while after some time the second mechanism becomes dominant.

As for Sezawa wave, the increase in the GO film thickness produced by water vapor adsorption leads to insignificant increase in the wave velocity (Table 1). This fact is attributed to less localization of the wave near the surface as compared with the Rayleigh wave [45]. As a result, for Sezawa wave in ZnO/Si structure the main sensing mechanism is every time the mass loading producing decrease in the wave velocity (Fig. 6b) [46], while in GO/ZnO/Si structure the main sensing mechanisms are the mass loading and the electric conductivity decreasing the wave velocity as well (Fig. 6d).

Calibration curves of the humidity sensors based on Rayleigh and Sezawa waves are linear in the range from RH = 20 to 98% (Fig. 7). The slope of the curve for Sezawa wave demonstrates record sensitivity of the sensor as compared both with Rayleigh wave in the same structure (Fig. 7) and with other prototypes known so far (Table 2). On

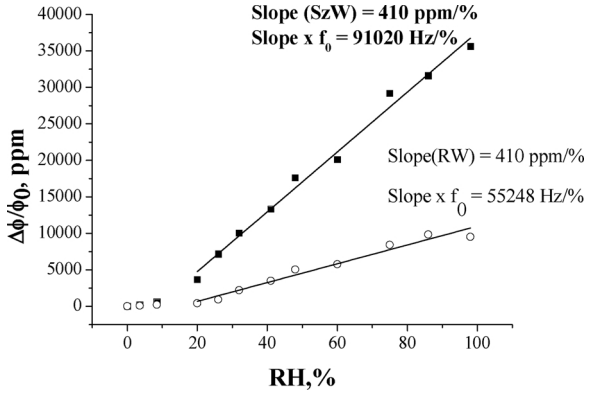

Fig. 7. Calibration curves of the humidity sensors based on Rayleigh(open circles) and Sezawa (black squares) waves in GO/ZnO/Si structure. Solid lines represent the fitting curves obtained by Origin 8,0 Programme.

Table 2
Comparison of the known humidity sensors based on the GO sorbent films.

Wave type	Materials	Humidity range, %RH	Resp./rec. time, s	Sens., kHz/%, RH	Ref.
SAW	Quartz + GO	5–100	n/a	1.54	[5]
SAW	ZnO/glass + GO	0.5–85	19/ < 1	53	[6]
Love wave	Si/SiO2 + GO	10–76	n/a	2.4	[17]
QSM	Quartz + GO	6.4–93.5	18/12	2.6	[20]
QSM	Quartz + GO/PEI	11.3–97.3	53/18	27.25	[22]
FBAR	Si/SiO2/ZnO + GO	5–83	n/a	25.5	[23]
A_0 Lamb wave	Flexible ZnO/PI + GO	10–85	22/5	22	[25]
S_0 Lamb wave	Flexible ZnO/PI + GO	10–85	16/5	35	[25]
Lamb wave	128Y-X + 90	0.03–75	87/50	80	[26]
Sezawa wave	ZnO/Si + GO	3.6–98	600/6	91	Present paper
Rayleigh wave	ZnO/Si + GO	3.6–98	600/6	6	Present paper

Table 3
Key performance parameters of the humidity sensor based on Sezawa wave propagating in GO/ZnO.Si structure developed in the paper.

Parameter	Values
Central frequency	222 MHz
Insersion loss	19.4 dB
Sensitivity tow. humidity	91020 Hz/%
Sensitivity tow/temperature	9050 Hz/%
Humidity range, RH	3.6–98%
Experimental accuracy	ΔRH = ± 0.1%
Resp./rec. times	600 s/6 s
Operation temperature	20 ± 5 °C

the other hand, the temperature instability of the Rayleigh wave sensor estimated from data [47] is lower (4100 Hz/°C) than that is for Sezawa wave device (9050 Hz/°C), while both values are much less than the sensitivity of the same waves towards humidity (55250 Hz/% and 91020 Hz/%, respectively). Therefore, the measurement accuracy for the temperature variations ± 1 °C is about ΔRH = ± 0.1%.

The key performance parameters of the humidity sensor developed in the paper are presented on Table 3.

5. Conclusion

Theoretical predictions and experimental verifications accomplished in the paper showed that Sezawa wave and GO/ZnO/Si structure provide an improved humidity sensor with better performance as compared with other prototypes based on the same film. The sensor has enhanced sensitivity (91 kHz/%) and linear response in the range 20–98%RH. For further improvements of the sensor performance an acoustic wave with stronger piezoelectric properties propagating in GO-based structure should be found.

Acknowledgments

The work has been partially supported by Russian Science Foundation Grant #15-19-20046-P in frame of development of humidity sensor and by Russian Foundation of Basic Research Grant #17-07-00750 in frame of theoretical analysis of multilayered structures.

References

[1] C. Caliendo, E. Verona, V.I. Anisimkin, Surface acoustic wave humidity sensors: a comparison between different types of sensitive membrane, Smart Mater. Struct. 6 (1997) 707–715.
[2] J. Devkota, P.R. Ohodnicki, D.W. Greve, SAW sensors for chemical vapors and gases, Sensors 17 (2017) 801.
[3] Y. Tang, Z. Li, J. Ma, L. Wang, J. Yang, B. Du, Q.K. Yu, X.T. Zu, Highly sensitive surface acoustic wave (SAW) humidity sensors based on sol-gel SiO_2 films: investigations on the sensing property and mechanism, Sens. Act. B: Chem. 215 (2015) 283–291.
[4] V.I. Anisimkin, I.M. Kotelyanslii, V.I. Fedosov, C. Cfliendo, P. Verardi, E. Verona, Real time characterization of elastic variations in palladium films produced by hydrogen adsorption, Proceed. IEEE Ultras. Symp. (1996) 293–297.
[5] S.M. Balashov, O.V. Balachova, F.A. Pavani, M.C.Q. Bazetto, M.G. de Almeida, Surface acoustic wave humidity sensors based on graphene oxide thin films deposited with the surface acoustic wave atomizer, ECS Trans. 49 (2012) 445–450.
[6] W. Xuan, M. He, N. Meng, X. He, W. Wang, J. Chen, T. Shi, T. Hasan, Z. Xu, Y. Xu, J.K. Luo, Fast response and high sensitivity ZnO-glass SAW humidity sensors using graphene oxide sensing layer, Sci. Rep. 4 (2014) 7206–7214.
[7] Y.J. Guo, J. Zhang, C. Zhao, P.A. Hu, X.T. Zu, Y.Q. Fu, Graphene/LiNbO3 surface acoustic wave device based relative humidity sensor, Optik 125 (2014) 5800–5802.
[8] F.S. Irani, B. Tunaboylu, SAW humidity sensor sensitivity enhancement via electrospraying of silver nanowires, Sensors 16 (2016) 2024.
[9] Y. Liu, H. Huang, L. Wang, D. Cai, B. Liu, D. Wang, Q. Li, T. Wang, Electrospun CeO_2 nanoparticles/PVP nanofibers based high-frequency surface acoustic wave humidity sensor, Sens. Act B: Chem. 223 (2016) 730–737.
[10] R. Rimeika, D. Ciplys, V. Poderys, R. Rotomskis, M.S. Shur, Fast-response and low-loss surface acoustic wave humidity sensor based on bovine serum albumin-gold nanoclusters film, Sens. Act. B: Chem. 239 (2017) 352–357.
[11] H.L. He, D.J. Li, J. Zhou, W.B. Wang, W.P. Xuan, S.R. Dong, H. Jin, J.K. Luo, High sensitivity humidity sensors using flexible surface acoustic wave devices made on nanocrystalline ZnO/polyimide substrates, J. Mater. Chem. C 1 (2013) 6210–6215.
[12] L. Blanc, A. Tetelin, C. Boissière, G. Tortissier, C. Dejous, D. Rebière, Love wave characterization of the shear modulus variations of mesoporous sensitive films during vapor sorption, IEEE Sens. J. 12 (2012) 1442–1449.
[13] J.K. Kwan, J.C. Sit, High sensitivity Love-wave humidity sensors using glancing angle deposited thin films, Sens. Act. B: Chem. 173 (2012) 164–168.
[14] Y.J. Guo, J. Zhang, C. Zhao, J.Y. Ma, H.F. Pang, P.A. Hu, F. Placido, D. Gibson, X.T. Zu, H.Y. Zu, Y.Q. Fu, Characterization and humidity sensing of ZnO/428 YX LiTaO3 Love wave devices with ZnO nanorods, Mater. Res. Bul. 48 (2013) 5058–5063.
[15] L. Wang, J. Liu, S. He, The development of Love wave-based humidity sensors incorporating multiple layers, Sensors 15 (2015) 8615–8623.
[16] Y. Wang, S.-Y. Zhang, L. Fan, X.-J. Shui, Y.-T. Yang, Surface acoustic wave humidity sensors based on (1120) ZnO piezoelectric films sputtered on R-sapphire substrates, Chin. Phys. Lett. 32 (2015) 086802.
[17] I. Nikolaou, H. Hallil, V. Conédéra, G. Deligeorgis, C. Dejous, D. Rebiere, Inkjet-printed graphene oxide thin layers on Love wave devices for humidity and vapor detection, IEEE Sens. J. 16 (2016) 7620–7627.
[18] M. Penza, G. Cassano, P. Aversa, D. Suriano, E. Verona, M. Benetti, D. Cannatà, F. Di Pietrantonio, W. Wlodarski, Thin film bulk acoustic resonator vapor sensors with single-Walled carbon nanotubes-based nanocomposite layer, Proceed. IEEE Sens. Conf. (2007) 185–188.
[19] X. Wang, B. Ding, J. Yu, M. Wang, F. Pan, A highly sensitive humidity sensor based on a nanofibrous membrane coated quartz crystal microbalance, Nanotechnology 21 (2010) 055502.
[20] Y. Yao, Z. Chen, H. Guo, Z. Wu, Graphene oxide thin film coated quartz crystal microbalance for humidity detection, Appl. Surf. Sci. 257 (2011) 7778–7782.
[21] Y. Yao, Y. Xue, Influence of the oxygen content on the humidity sensing properties of functionalized graphene films based on bulk acoustic wave humidity sensors, Sens. Act. B: Chem. 222 (2016) 755–762.
[22] Z. Yuan, H. Tai, Z. Ye, C. Liu, G. Xie, X. Du, Y. Jiang, Novel highly sensitive QSM humidity sensor with low hysteresis based on graphene oxide (GO)/poly(ethyleneimine) layered film, Sens. Act. B: Chem. 234 (2016) 145–154.
[23] W. Xuan, M. Cole, J.W. Gardner, S. Thomas, F.-H. Villa-Lopez, X. Wang, S. Dong, J.A. Luo, A film bulk acoustic resonator oscillator based humidity sensor with graphene oxide as the sensitive layer, J. Micromech. Microeng. 27 (2017) 055017.
[24] W. Liu, H. Qu, J. Hu, W. Pang, H. Zhang, X. Duan, A highly sensitive humidity sensor based on ultrahigh-frequency microelectromechanical resonator coated with nano-assembled polyelectrolyte thin films, Micromachines 8 (2017) 116.
[25] W. Xuan, X. He, J. Chen, W. Wang, X. Wang, Y. Xu, Z. Xu, Y.Q. Fuc, J.K. Luo, High sensitivity flexible Lamb-wave humidity sensors with a graphene oxide sensing layer, Nanoscale 7 (2015) 7430–7436.
[26] I.E. Kuznetsova, V.I. Anisimkin, S.P. Gubin, S.V. Tkachev, V.V. Kolesov, V.V. Kashin, B.D. Zaitsev, A.M. Shikhabudinov, E. Verona, S. Sun, Super high sensitive plate acoustic wave humidity sensor based on graphene oxide film, Ultrasonics 81 (2017) 135–139.
[27] N. Yamazoe, Y. Shimizu, Humidity sensors: principles and applications, Sens. Act. 10 (1986) 379–398.
[28] Z. Chen, C. Lu, Humidity sensors: a review of materials and mechanisms, Sens. Lett. 3 (2005) 274–295.
[29] T. Hyodo, K. Urata, K. Kamada, Y. Shimizu, Semiconductor-type SnO2-based NO2

sensors operated at room temperature under UV-light irradiation, Sens. Act. B: Chem. 253 (2017) 630–640.
[30] D. Ciplis, R. Rimeika, V. Chivukula, M.S. Shur, J.H. Kim, J.M. Xu, Surface acoustic waves in graphene structures: response to ambient humidity, IEEE Sensors Conf. (2010) 785–788.
[31] J. Wei, Z. Zang, Y. Zhang, M. Wang, J. Du, X. Tang, Enhanced performance of light-controlled conductive switching in hybrid cuprous oxide/reduced graphene oxide (Cu2O/rGO) nanocomposites, Opt. Lett. 42 (2017) 911–914.
[32] Z. Zang, X. Zeng, M. Wang, W. Hu, C. Liu, X. Tang, Tunable photoluminescence of water-soluble AgInZnS-graphene oxide (GO) nanocomposites and their application in-vivo bioimaging, Sens. Act. B: Chem. 252 (2017) 1179–1186.
[33] B.A. Auld, Acoustic Fields and Waves in Solids vol. 2, Wiley, New York, 1973.
[34] A.A. Oliner, Acoustic Surface Waves, in: Topics in Applied Physics, 24 (1978), Chap. 2, Springer-Verlag, Berlin.
[35] B.D. Zaitsev, I.E., Kuznetsova, S.G., Joshi, I.A. Borodina, Shear horizontal acoustic waves in piezoelectric plates bordered with conductive liquid, IEEE Trans. on Ultras., Ferroel. and Freq. Contr. 48 (2001) 627–631.
[36] I.E. Kuznetsova, V.V. Kolesov, B.D. Zaitsev, S.V. Tkachev, V.V. Kashin, A.M. Shikhabudinov, A.S. Fionov, S.P. Gubin, S. Sun, Structural, electrical and acoustical properties of graphene oxide films for acoustoelectronic applications, Phys. Stat. Solidi A. (2017) 160757.
[37] Y. Zhu, D.K. James, J.M. Tour, New routes to graphene, graphene oxide and their related applications, Adv. Mater. 24 (2012) 4924–4955.
[38] S.V. Tkachev, A.V. Buslaeva, I.V. Laure, S.P. Gubin, Reduced graphene oxide, Inorg. Mater 48 (2012) 796–802.
[39] V.A. Smirnov, N.N. Denisov, A.E. Ukshe, Yu.M. Shul'ga, Effect of humidity on the conductivity of graphite oxide during its photoreduction, High Energy Chem. 47 (2013) 242–246.
[40] G. Karlotti, D., Fioretto, L., Palmieri, G., Socino, L., Verdini, E. Verona, Brilloin Scattering by surface acoustic modes for elastic characterization of ZnO films, IEEE Trans. on Ultras., Ferroel. and Freq. Contr. 38 (1991) 56–60.
[41] A.A. Mohanan, Md.S. Islam, S.H. Md Ali, R. Parthiban, N. Ramakrishnan, Investigation into mass loading sensitivity of Sezawa wave mode-based surface acoustic wave sensors, Sensors 13 (2013) 2164–2175.
[42] X.Y. Du, Y.Q. Fu, S.C. Tan, J.K. Luo, A.J. Flewitt, W.I. Milne, D.S. Lee, N.M. Park, J. Park, Y.J. Choi, S.H. Kim, S. Maeng, ZnO film thickness effect on surface acoustic wave modes and acoustic streaming, Appl. Phys. Lett. 93 (2008) 094105.
[43] A.J. Slobodnik, E.D. Conway, R.T. Delmonico, Microwave Acoustic Handbook, (1973) (AFCRL-TR-73-0597).
[44] V.B. Raj, H. Singh, A.T. Nimal, M.U. Sharma, M. Tomar, V. Gupta, Distinct detection of liquor ammonia by ZnO/SAW sensor: study of complete sensing mechanism, Sens. Act. B: Chem. 238 (2017) 83–90.
[45] A. Talbi, F. Sarry, L. Le Brizoual, M. Elhakiki, O. Elmazria, P. Alnot, Pressure sensitivity of Rayleigh and Sezawa wave in ZnO/Si(001) structures, Proc. IEEE Ultras. Symp. 1-2 (2003) 1338–1341.
[46] M. Prasad, V. Sahula, V.K. Khanna, Long-term effects of relative humidity on the performance of zno-based mems acoustic sensors, IEEE Trans. Dev. Mater. Rel. 14 (2014) 778–780.
[47] S. Ono, K. Wasa, S. Hayakawa, Surface-acoustic-wave properties in ZnO-SiO_2-Si layered structure, Wave Electronics 3 (1977) 35–49.

Iren E. Kuznetsova was born in Petropavlovsk-Kamchatsky, Russia on July 14, 1966. She graduated from Saratov State University in 1988 (physics of plasma) and received the Master's degree. In 1996, she received the Degree of Candidate of Sciences (Physics-Mathematics) (Ph.D.) from Saratov State University. In 2004 she has received the Doctor of Science diploma. Since 1988 and until present time, she has been working at the Kotelnikov Institute of Radio Engineering and Electronics of the Russian Academy of Sciences. She is Main Scientific Researcher. Since 1996 and until 1999 she worked at Saratov State University as part-time Associated Professor. Since 2004 until 2010 she has been working as part-time Professor at Saratov State Technical University. From 1999 until 2002 she worked at Marquette University, as Visiting Research Scientist. Currently, Iren E. Kuznetsova deals with the investigation of the bulk, surface and plate acoustic waves propagating in piezoelectric materials and the development of various devices and sensors based on this basis. She is engaged in the theoretical investigation of propagation of acoustic waves in conducting and viscous liquids. She has significant experience in numerical calculations of acoustic wave characteristics in various materials and structures. Prof. Kuznetsova has about 130 publications in Russia and abroad. She is Professor of Russian Academy of Science.

Vladimir I. Anisimkin was born in Uzbekistan, USSR, on August 11, 1948. In 1972, he received his degree in physics at the Moscow State University and joined the Institute of Radioengineering and Electronics, Russian Academy of Sciences, where he is now a principal researcher. He received his Ph.D. and Doctor of Sciences degrees in physics and mathematics from the same institute in 1977 and 1990, respectively. His research interests are concentrated on surface acoustic waves, thin solid films, and acoustic wave sensors for environmental control, chemistry, biology, and medicine. From 1987–2007, he engaged in fruitful scientific cooperation with the Institute of Acoustics O. M. Corbino, CNR, Italy; research center CNRSM, Italy; and the Industrial Technology Research Institute, Hsinchu, Taiwan. He has authored or coauthored about 100 papers and 10 patents of the Russian Federation. He has been an IEEE member since 1994.

Vladimir V. Kolesov was born in Moscow, Russia on June 27, 1951. He graduated from Moscow State University in 1974 (physics) and received the Master's degree. In 1980, he received the Degree of Candidate of Sciences (Physics- Mathematics) (Ph.D.) from Moscow State University. Now he is Head of Laboratory in Kotelnikov Institute of Radio Engineering and Electronics of RAS. His scientific interests are (i) Radio physics & Physical Electronics, (ii) Precision Measurements, Measurement of the weak microwave signals, Application of microwave power in Biology and Medicine, (iii) Nanoelectronics, Nanotechnology, Molecular & Bio-electronics, Information Technologies and Application of Nonlinear Dynamic Chaos in telecommunication systems. He is Scientific Deputy Chiefs of journal "Radiotekhnika» ISSN 0033-8486 and Scientific journal 'RENSIT: Radioelektronika. Nanosistemy. Informatsionnye Tekhnologii' ISSN 2218–3000. He has about 100 publications in Russia and abroad.

Vadim V. Kashin was born in Moscow, Russia on August 23, 1968. He graduated from Moscow State University in 1993 (physics) and received the Master's degree. Now he is a PHD student of Kotelnikov Institute of Radio Engineering and Electronics of RAS. As well he is a researcher in Kotelnikov Institute of Radio Engineering and Electronics of RAS since 1993. His current research interests are caracterization of nanocarbon materials and development of bionanosensors. He has about 15 publications in Russia and abroad.

Victor A. Osipenko was born in Smolensk, Russia on September 18, 1951. He graduated from Leningrad Electro-Technical Institute nm.V.I.Lenin in 1975 (physics) and received the Master's degree. In 1979, he received the Degree of Candidate of Sciences (Physics-Mathematics) (Ph.D.) from Leningrad Electro-Technical Institute nm.V.I.Lenin. Now he is Senior Research Scientist in AO NII ELPA. His scientific interests are techology of thin film deposition (ZnO, GaN), development of microwave acoustic sensors,- development of signal processing devices. He has about 10 publications in Russia and abroad.

Sergei P. Gubin DrSc. (Chem.), Professor, Laboratory of Nanomaterials Chemistry, N.S. Kurnakov Institute of General and Inorganic Chemistry, Russian Academy of Sciences, Moscow. Sergey Pavlovich Gubin was born on 08/05/1937 in Moscow, Russia. Graduated from MSU, Chemical Dept. in 1959, Degree of Chemist (M. Sc.). Candidate of Chemical Sciences (Ph. D.) (1962), Doctor of Chemical Sciences (Highest Degree) (1971), Professor (1980). Career history: Laboratory of Organometallic Institute of Organoelement Compounds Chemistry, Senior Recearcher (1962–1977), Institute of Chemistry and Chemical Technology, Syberian Branch, Academy of Sciences of USSR, Krasnoyarsk, Director (1977–1980), Institute of Inorganic Chemistry Syberian Branch, Academy of Sciences of USSR, Novosibirsk, Director (1980–1983), Laboratory of Polynuclear and Cluster Compounds, N.S. Kurnakov Institute of General and Inorganic Chemistry, RAS, Moscow, Head of Laboratory (1983–2002), Laboratory of Nanomaterials Chemistry, N.S. Kurnakov Institute of General and Inorganic Chemistry, RAS, Moscow, Head of laboratory (2002-present time). Main scientific interests: Cluster chemistry; synthesis, reactivity, structure; heterometalic clusters redox properties, stereochemistry; Nano-materials, nano-particles and clusters, preparation, properties, stabilisation; nanoparticles in matrix; magnetic properties of nanomaterials, nano-electronics, graphen, nano-ink. Prof. Gubin S.P. has about 500 scientific papers in journails, 30 patents and 5 books

Sergei V. Tkachev was born in Kazan, Russia on December 20, 1986. He graduated from Moscow State University in 2008 (Chemistry) and received the Master's degree. In 2011, he received the Degree of Candidate of Sciences (Chemistry) (Ph.D.) from Moscow State University. Now she is Senior Research Scientist in N.S. Kurnakov Institute of General and Inorganic Chemistry, Russian Academy of Sciences, Moscow. His scientific interests include Nano-materials, nano-particles and clusters, preparation, properties, stabilisation; nanoparticles in matrix; magnetic properties of nanomaterials, nano-electronics, graphen, nano-ink. He has about 30 publications in Russia and abroad.

Enrico Verona received the Doctor degree in electronic engineering from the University of Rome "La Sapienza" in 1973. After working for a short period in the industry (SeleniaS.p.A.) he joined the "O.M.Corbino" Institute of Acoustics of the Italian National Research Council (CNR)where he has been leading the Acousto-Optics and Surface Acoustic Waves Group since 1983. From 1995–2001 he has been the Director of the"O.M.Corbino" Institute. E. Verona has been VisitingProfessor at the Department of Electronics of the University of Rome "La Sapienza", and in1989/90Professor of Electro-acoustics at the University of Perugia. Presently he is Associate Researcher at the Institute of Photonics and Nanotechnology of CNR. His research interests include physical acoustics, acoustoelectric and acousto-optic devices, surface acoustic waves, nonlinear acoustics, thin piezoelectric films, and SAW-based sensors.

Professor Shaorong Sun was born in 1954 in China. He is Professor and Deputy dean of Business school, University of Shanghai for Science and Technology. President of Engineering Management Society of Shanghai. Chairman of International Conference on Behavioral Operation Management. Leader of five foundation programs of National Natural Science Foundation of China (NFSC). Research interests: Management science;Computor science. In 1987, he was admitted to East China Normal University as a master degree in computer retrieval. In 1989, he was admitted to East China Normal University for Management Science, and graduated in 1992. His work experience is: 1992: Lecturer, 1994: Associate Professor, 1998: Professor, 2000: Doctoral Supervisor. His scientific interests include information retrieval; information science; game theory; institutional economics; engineering management; institution design.

Anastasia S. Kuznetsova was born in Saratov, Russia on September 19, 1986. She graduated from Saratov State University in 2008 (physics) and received the Master's degree. In 2011, she received the Degree of Candidate of Sciences (Physics- Mathematics) (Ph.D.) from Saratov State University. Now she is Senior Research Scientist in Kotelnikov Institute of Radio Engineering and Electronics of RAS. Her scientific interests include theoretical study of acoustic waves in piezoelectric plates and structures and theoretical investigation of characteristic of acoustic waves in piezoelectric plates contacting with liquids. She has about 30 publications in Russia and abroad.